Design of Switched Model Predictive Control Algorithms for a Dual-Hormone Artificial Pancreas

Boiroux, Dimitri; Bátora, Vladimír; Mahmoudi, Zeinab; Jørgensen, John Bagterp

Published in:
I F A C Workshop Series

Link to article, DOI:
10.1016/j.ifacol.2018.11.647

Publication date:
2018

Document Version
Publisher's PDF, also known as Version of record

Available online at www.sciencedirect.com

ScienceDirect

IFAC PapersOnline CONFERENCE PAPER ARCHIVE

IFAC PapersOnLine 51-27 (2018) 174–179

Design of Switched Model Predictive Control Algorithms for a Dual-Hormone Artificial Pancreas ⋆

Dimitri Boiroux * **Vladimír Bátora** ** **Zeinab Mahmoudi** * **John Bagterp Jørgensen** *

* *Department of Applied Mathematics and Computer Science, Technical University of Denmark, DK-2800 Kgs. Lyngby, Denmark.*
** *Ekom spol. s.r.o., Priemyselna 18, 921 01 Piestany, Slovakia.*

Abstract: In this paper, we evaluate the closed-loop performance of two switching strategies for a dual-hormone artificial pancreas (AP). The dual-hormone AP administers insulin and glucagon subcutaneously. Since insulin and glucagon have opposite effects, we want to avoid simultaneous injections of these two hormones. To handle non-simultaneous injections of insulin and glucagon, we compare model predictive control (MPC) algorithms using a hysteresis switch between insulin and glucagon controllers with a multiple-input single-output (MISO) formulation. Although the closed-loop performance of these two control strategies is similar, the hysteresis switch is preferable due to (i) its greater flexibility in control design and tuning and (ii) a more straightforward way to avoid simultaneous injections of insulin and glucagon.

Keywords: Dual hormone artificial pancreas, diabetes technology, type 1 diabetes, model predictive control

1. INTRODUCTION

The artificial pancreas (AP) has the potential to automatically provide insulin doses for patients with T1D (Trevitt et al. (2015); Haidar (2016)). A major concern for an AP is safety and in particular its ability to avoid insulin-induced hypoglycemia (low blood glucose). One way to prevent hypoglycemia or to reduce the duration of hypoglycemic events is to include glucagon in the AP. An AP able to administer insulin and glucagon is referred to in this paper as a dual-hormone AP while in other works it is referred to as a bihormonal AP or a (bihormonal) bionic pancreas. Current versions of the dual-hormone AP consist of a CGM, a control algorithm, and two pumps for insulin and glucagon administration.

Regular glucagon is not stable in an aqueous liquid formulation under standard conditions and has to be dissolved immediately before use. Therefore, its use has been limited to hypoglycemia rescue kits. Stable liquid formulations of glucagon or glucagon analogues have the potential to be used in pumps (Castle et al. (2016); Zealand Pharma - Dasiglucagon multiple-dose pump use (2018)). Results from simulations and clinical studies show that a dual-hormone AP can increase the safety of the glucose control and provide tighter regulation than a single-hormone AP without increasing the risk of hypoglycemia (Russell et al. (2014); Haidar et al. (2017)).

The first clinical studies of the dual-hormone AP by Russell et al. (2014) allowed simultaneous administration of insulin and glucagon. These studies showed that a dual-hormone AP reduces the time spent in hypoglycemia, but the total amount of administered glucagon was for some patients higher than the rescue dose (1 mg). In this study, a number of patients reported nausea and vomiting, which are known side effects of an excessive glucagon administration. In the work from Haidar et al. (2015), the insulin delivery was suspended before delivering glucagon.

To avoid adverse effects, it is therefore crucial to design control strategies that avoid unnecessary injections of glucagon. In our previous work, we considered a hysteresis switching strategy between insulin and glucagon (Bátora et al. (2014); Bátora et al. (2015); Boiroux et al. (2015)). MPC strategies with switching for more general applications have been theoretically studied (Bemporad and Morari (1999); Dua et al. (2002); Mhaskar et al. (2005)).

In this paper, we consider two strategies to handle switching. The first strategy uses a hysteresis switch based on the measured glucose concentration. The second strategy uses a multiple input single output (MISO) formulation where a penalty on glucagon injections reduces the risk of simultaneous injection of insulin and glucagon.

This paper is structured as follows. Section 2 presents the continuous-time transfer function model. Section 3 describes the optimal control problem (OCP) solved at every time sample. In Section 4, we discuss the comparison between the hysteresis switch of MPC and the MISO MPC algorithms using 30-hour simulations on three virtual patients. Section 5 summarizes the main contributions of this paper.

⋆ This paper is funded by The Danish Diabetes Academy supported by the Novo Nordisk Foundation.

10.1016/j.ifacol.2018.11.647

2. MODELING OF THE GLUCOSE-INSULIN-GLUCAGON DYNAMICS

This section presents a control-relevant linear model for the glucose concentration measured by a CGM. The model is obtained through a discretization of a transfer function model describing insulin and glucagon action on the interstitial glucose concentration. The model has a deterministic part and a stochastic part. The deterministic part describes the effect of subcutaneously (sc) injected insulin and glucagon, $u_I(t)$ and $u_G(t)$, on glucose concentration. The stochastic part describes the effect of other unknown factors affecting the human metabolism and the interstitial glucose concentration.

2.1 Transfer function models

We consider a continuous-time model of the form

$$Y(s) = Y_D(s) + Y_S(s) = G(s)U(s) + H(s)E(s). \quad (1)$$

$Y_D(s)$ represents the deterministic part of the model and $Y_S(s)$ the stochastic part of the model. The term $Y_D(s) = G(s)U(s)$ in (1) models the effect of the manipulated variables, $U(s)$ (insulin and glucagon), on the output (sc CGM glucose concentration). Thus, the deterministic part, $Y_D(s)$, can be reformulated as

$$\begin{aligned} Y_D(s) &= [G_I(s)\ G_G(s)] \begin{bmatrix} U_I(s) \\ U_G(s) \end{bmatrix} \\ &= G_I(s)U_I(s) + G_G(s)U_G(s). \end{aligned} \quad (2)$$

$G_I(s)$ and $G_G(s)$ represent the transfer functions from insulin/glucagon to sc glucose. $U_I(s)$ and $U_G(s)$ are the Laplace transforms of the insulin injection, $u_I(t)$, and the glucagon injection, $u_G(t)$.

The term $Y_S(s) = H(s)E(s)$ in (1) constitutes the stochastic part of the model. A significant part of $Y_S(s)$ is the significant model-patient mismatches present in the low order models describing the effect of sc injected insulin and sc injected glucagon on sc glucose. While the disturbance model $H(s)$ can be parametrized in continuous time, we do not do so in this paper (Hagdrup et al. (2016)). Instead, we identify the disturbance model in discrete-time as in Boiroux et al. (2018).

2.2 Parameter identification

In this paper, the gains, K_I [(mmol/L)/(U/min)] and K_G [(mmol/L)/(pg/min)], and the time constants, τ_I [min] and τ_G [min], are identified by least-squares fitting of the insulin and glucagon impulse responses. Based on our previous work (Boiroux et al. (2015)), we choose second-order transfer function models in the form

$$G_i(s) = \frac{K_i}{(\tau_i s + 1)^2}, \quad i \in \{I, G\}. \quad (3)$$

2.3 Realization, filtering and prediction

After discretization, we represent the continuous-time transfer function model as the following discrete-time state space model in innovation form

$$x_{k+1} = Ax_k + B_I u_{I,k} + B_G u_{G,k} + K\varepsilon_k, \quad (4a)$$
$$y_k = Cx_k + \varepsilon_k. \quad (4b)$$

The state-space matrices (A, B_I, B_G, K, C) are obtained using an observer canonical realization. The innovation of the discrete-time state space model (4) is

$$\varepsilon_k = y_k - C\hat{x}_{k|k-1}, \quad (5)$$

and the corresponding predictions are (Jørgensen et al. (2011))

$$\hat{x}_{k+1|k} = A\hat{x}_{k|k-1} + B\hat{u}_{k|k} + K\varepsilon_k, \quad (6a)$$
$$\hat{x}_{k+1+j|k} = A\hat{x}_{k+j|k} + B\hat{u}_{k+j|k}, \quad j = 1, \dots, N-1, \quad (6b)$$
$$\hat{y}_{k+j|k} = C\hat{x}_{k+j|k}, \quad j = 1, \dots, N, \quad (6c)$$

where $B = [B_I\ B_G]$ and $\hat{u}_{k|k} = \left[\hat{u}_{I;k|k}\ \hat{u}_{G;k|k}\right]^T$. The innovation (5) and the predictions (6) constitute the feedback and the predictions in the model predictive controller described in the next section.

3. OPTIMAL CONTROL PROBLEM

At each sample time, the controller computes the insulin micro-bolus and/or glucagon infusion rate by solving the convex quadratic program

$$\min_{\{u_{I,G;k+j|k}, \eta_{k+j+1|k}\}_{j=0}^{N-1}} \quad \phi, \quad (7a)$$

$$\begin{aligned}
s.\,t.\quad & \hat{x}_{k+1|k} = A\hat{x}_{k|k-1} + B_I u_{I;\,k|k} + \\
& \qquad B_G u_{G;\,k|k} + Ke_k, && (7b)\\
& \hat{y}_{k+1|k} = C\hat{x}_{k+1|k}, && (7c)\\
& \hat{x}_{k+1+j|k} = A\hat{x}_{k+j|k} + B_I u_{I;\,k+j|k} + \\
& \qquad B_G u_{G;\,k+j|k}, && j \in \mathcal{N}_1, \quad (7d)\\
& \hat{y}_{k+1+j|k} = C\hat{x}_{k+1+j|k}, && j \in \mathcal{N}_1, \quad (7e)\\
& u_{I;\min} \le u_{I;\,k+j-1|k} \le u_{I;\max}, && j \in \mathcal{N}_0, \quad (7f)\\
& u_{G;\min} \le u_{G;\,k+j-1|k} \le u_{G;\max}, && j \in \mathcal{N}_0, \quad (7g)\\
& \hat{y}_{k+j|k} \ge y_{\min} - \hat{\eta}_{k+j|k}, && j \in \mathcal{N}_0, \quad (7h)\\
& \hat{y}_{k+j|k} \le y_{\max} + \hat{\eta}_{k+j|k}, && j \in \mathcal{N}_0, \quad (7i)\\
& \hat{\eta}_{k+j|k} \ge 0, && j \in \mathcal{N}_0, \quad (7j)
\end{aligned}$$

where $\mathcal{N}_0$={1,...,N}, $\mathcal{N}_1$={1,...,N-1}. The objective function, ϕ, is

$$\begin{aligned}
\phi = \frac{1}{2}\sum_{j=0}^{N-1} & \overbrace{\|\hat{y}_{k+1+j|k} - r_{k+1+j|k}\|^2 + \gamma\|\hat{\eta}_{k+1+j|k}\|^2}^{\text{Glucose penalty function}} \\
& + \frac{1}{2}\sum_{j=0}^{N-1} \overbrace{\lambda_I\|\Delta u_{I;k+j|k}\|^2 + \lambda_G\|u_{G;k+j|k}\|^2}^{\text{Regularization term}}. \quad (8)
\end{aligned}$$

We set the maximal glucagon infusion rate, $u_{G;\max}$, to a large value (7g). Compared to our previous controller design (Bátora et al. (2014); Bátora et al. (2015); Boiroux et al. (2015)), we penalize here the 2-norm of glucagon injections instead of glucagon variations. This formulation penalizes the simultaneous administration of insulin and glucagon, and more generally avoids unnecessary glucagon injections.

3.1 Hysteresis switch

One strategy to avoid simultaneous injections of insulin and glucagon is based on relay switching with hysteresis. The glucagon controller is activated when the measured glucose concentration falls below 4.5 mmol/L (81 mg/dL). At the same time the insulin MPC is switched off. The insulin MPC is switched back on only after the measured glucose concentration rises above 5 mmol/L (90

Table 1. Individualized controller parameters.

Symbol	Unit	Patient 1	Patient 2	Patient 3
BW	kg	85.0	68.6	94.8
IC	U/g	0.166	0.363	0.333
K_I	$\frac{\text{mmol/L}}{\text{U/min}}$	-9.49	-3.76	-3.91
τ_I	min	220	170	240
$u_{I;b}$	mU/min	6.0	9.7	14.5
$\bar{y}_I$	mmol/L	5.5	5.5	5.5
$y_{I;min}$	mmol/L	4.0	4.0	4.0
$y_{I;max}$	mmol/L	10.0	10.0	10.0
K_G	$\frac{\text{mmol/L}}{\mu\text{g/min}}$	0.0403	0.0221	0.0171
τ_G	min	165	120	155
$\bar{y}_G$	mmol/L	5.0	5.0	5.0
$y_{G;min}$	mmol/L	4.0	4.0	4.0
$y_{G;max}$	mmol/L	6.0	6.0	6.0

mg/dL). When the hysteresis switch is used, the glucagon injections, $u_{G;k+j|k}$, are set to 0 in (7) when the insulin controller is active. Conversely, we set the insulin injection rates to $-u_{I;b}$ in (7) when the glucagon controller is active. Since the insulin infusion rates are expressed in terms of deviation variables from the steady state, this corresponds to a shutdown of the insulin pump. For further information about the practical implementation of the switching based on hysteresis, the reader is referred to Bátora et al. (2014); Bátora et al. (2015).

3.2 Mealtime bolus calculation

The insulin mealtime bolus calculation utilizes information about the insulin-to-carbohydrate ratio, IC (U/g), and the ingested meal size, CHO (g). We estimate the IC from the insulin sensitivity factor and the patient's response to a defined amount of carbohydrates ingested. We compute the bolus size in the following way

$$Bolus = CHO \cdot IC. \tag{9}$$

In some of our previous work, we showed that the optimal insulin administration following a meal is a bolus followed by a suspension of insulin (Boiroux et al. (2010)). Similar results have been established for meals with low-fat content (Srinivasan et al. (2014)). In this paper, we suspend the insulin infusion for two hours after mealtime. This strategy is also known as a super-bolus, see eg. Rossetti et al. (2012); Boronat et al. (2015).

4. NUMERICAL RESULTS

We test the controllers for three simulated patients using the parameters for the glucose-insulin-glucagon simulation model described in the Appendix. The daily meal regimen consists of three bolused meals and two unbolused snacks. The meal sizes are adjusted according to the body weight of the patient. In all the simulations, we use the same CGM noise realization for comparison purposes.

Fig. 1 shows the glucose and insulin traces for Patient 3 over a 30-hour simulation. The MISO and hysteresis control strategies show very similar performances. It must be pointed out that the MISO formulation has a penalty on glucagon administration. It is used to discourage simultaneous injection of insulin and glucagon.

Table 2 reports the closed-loop performance of the two different control strategies for the three patients. In the

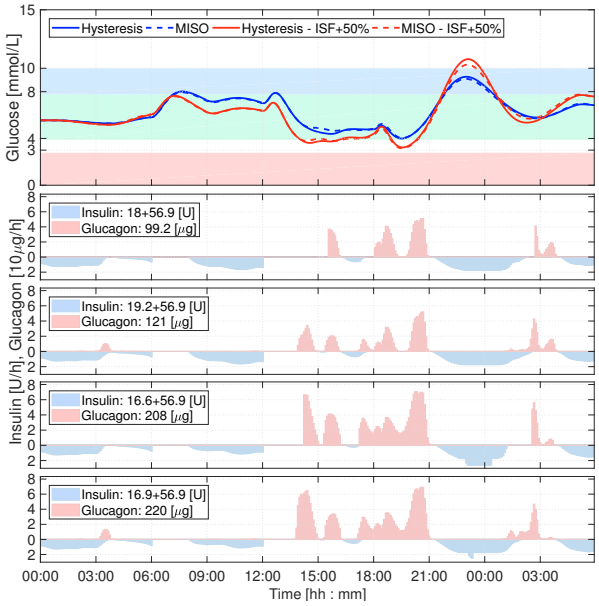

Fig. 1. Simulated closed-loop performance comparison of two different dual-hormone APs for Patient 3. From top to bottom: Hysteresis - nominal insulin sensitivity, MISO - nominal insulin sensitivity, Hysteresis - increased insulin sensitivity, MISO - increased insulin sensitivity.

case where the insulin sensitivity is not increased, we did not observe any hypoglycemia (BG≤3.9 mmol/L). For the case where the insulin sensitivity is increased by 50%, the MISO control strategy shows a marginally better performance compared to the hysteresis switching strategy for 2 out of the 3 patients. For Patient 3, the hysteresis switch showed less severe hypoglycemia (BG≤3.3 mmol/L) than the MISO control strategy. This is possibly due to the ability to administer glucagon sufficiently in advance of a predicted hypoglycemic event. In summary, the switching strategy based on hysteresis uses less insulin and glucagon than the MISO control design in every case for a comparable performance.

A switching strategy between the insulin and glucagon controller is more flexible than the MISO controller design. It allows different administration strategies, for instance an insulin pump combined with a glucagon pen (Reiter et al. (2016)) or different control algorithms for insulin and glucagon such as in Castle et al. (2010); Russell et al. (2012). It is also possible to design different MPC strategies for insulin and glucagon, including different models, glucose setpoints, or different thresholds for soft constraints.

However, the model does not take into account the inhibitory action of insulin on glucagon secretion. High insulin-on-board levels reduce the effectiveness of administered glucagon (El Youssef et al. (2014)). Some other physiological models, including the model developed by Man et al. (2014) and the more recent model developed by Wendt et al. (2016, 2017), take this into account. Therefore, larger *in silico* and clinical studies will be needed to further design dual-hormone control strategies.

Table 2. Percentage of time spent in different glucose ranges, administered basal insulin and glucagon.

		Nominal insulin sensitivity		Insulin sensitivity increased by 50%	
		MISO	Hysteresis	MISO	Hysteresis
Patient 1	$G > 10.0$ mmol/L (%)	0.00	0.00	0.00	0.00
	$3.9 \leq G \leq 10.0$ mmol/L (%)	100.0	100.0	96.7	94.7
	$3.9 \leq G \leq 7.8$ mmol/L (%)	90.8	90.6	91.1	89.7
	$G < 3.9$ mmol/L (%)	0.00	0.00	3.3	5.3
	$G < 3.3$ mmol/L (%)	0.00	0.00	0.00	0.00
	$G < 2.8$ mmol/L (%)	0.00	0.00	0.00	0.00
	Total basal insulin administered (U)	7.1	5.85	6.6	4.9
	Total glucagon administered (μg)	64.9	31.4	148.5	93.4
Patient 2	$G > 10.0$ mmol/L (%)	0.00	0.00	0.00	0.00
	$3.9 \leq G \leq 10.0$ mmol/L (%)	100.0	100.0	91.1	90.8
	$3.9 \leq G \leq 7.8$ mmol/L (%)	92.2	92.2	86.7	86.1
	$G < 3.9$ mmol/L (%)	0.00	0.00	8.9	9.2
	$G < 3.3$ mmol/L (%)	0.00	0.00	0.00	1.9
	$G < 2.8$ mmol/L (%)	0.00	0.00	0.00	0.00
	Total basal insulin administered (U)	8.6	7.4	8.4	6.6
	Total glucagon administered (μg)	52.0	31.0	133.1	106.1
Patient 3	$G > 10.0$ mmol/L (%)	0.00	0.00	3.1	4.4
	$3.9 \leq G \leq 10.0$ mmol/L (%)	100.0	100.0	87.5	84.2
	$3.9 \leq G \leq 7.8$ mmol/L (%)	87.2	86.4	81.1	78.9
	$G < 3.9$ mmol/L (%)	0.00	0.00	9.4	11.4
	$G < 3.3$ mmol/L (%)	0.00	0.00	2.5	1.9
	$G < 2.8$ mmol/L (%)	0.00	0.00	0.00	0.00
	Total basal insulin administered (U)	19.2	18.0	16.8	16.6
	Total glucagon administered (μg)	121.3	99.2	219.8	207.9

5. CONCLUSION

This paper provides a comparison between switching strategies for a dual-hormone AP. The numerical results suggest that the closed-loop performance of a hysteresis switching strategy and a MISO control design is similar. However, the MISO control design has several drawbacks. The main drawback of MISO control design is the lack of flexibility in design. It is also more difficult to completely avoid simultaneous injections of insulin and glucagon using a MISO design. The results presented in this paper could also apply to other applications where switching between several inputs may occur. Generally, simple switching strategies can be implemented without compromizing the performance of the control algorithm.

Appendix A. SIMULATION MODEL

The model proposed by Herrero et al. (2013) has been used for all the simulations in this paper. This model simulates the effects of meals intake, subcutaneously administered insulin and glucagon. We added the CGM model from Breton and Kovatchev (2008).

A.1 Extended model of glucose dynamics

The glucose dynamics are described by the following system of differential equations

$$\dot{G}(t) = -[S_G + X(t) - Y(t)]G(t) + S_G G_b + \frac{D_2(t)}{t_G V}, \tag{A.1a}$$

$$\dot{X}(t) = -p_2 X(t) + p_2 S_I [I(t) - I_b], \tag{A.1b}$$

$$\dot{Y}(t) = -p_3 Y(t) + p_3 S_N [N(t) - N_b], \tag{A.1c}$$

where $G(t)$ [mg/dL] is the plasma glucose concentration, $I(t)$ [μU/dL] is the plasma insulin, and $N(t)$ [pg/dL] is the plasma glucagon concentration. $X(t)$ [min^{-1}] and $Y(t)$ [min^{-1}] represent the insulin and glucagon action on glucose production. S_G [min^{-1}] is the fractional glucose effectiveness describing how glucose per se promotes its own disposal and inhibits its production. S_I [$\text{min}^{-1}/(\mu\text{U/mL})$] and S_N [$\text{min}^{-1}/(\text{pg/mL})$] are the insulin and glucagon sensitivities. p_2 [min^{-1}] and p_3 [min^{-1}] are inverses of time constants describing the dynamics of insulin and glucagon action. V [dL/kg] is the glucose distribution volume and $R_a(t) = D_2(t)/t_G$ [mg/min/kg] is the rate of appearance of glucose in plasma following a meal ingestion. The subscript b denotes basal states.

A.2 Gastrointestinal absorption model

The model incorporates the two-compartment gastrointestinal absorption subsystem from Hovorka et al. (2004)

$$\dot{D}_1(t) = -\frac{1}{t_G} D_1(t) + A_G D_G, \tag{A.2a}$$

$$\dot{D}_2(t) = \frac{1}{t_G}(D_1(t) - D_2(t)). \tag{A.2b}$$

$D_1(t)$ [mg/kg] describes the glucose in the first compartment and $D_2(t)$ [mg/kg] is the glucose in the second compartment. A_G [-] is the carbohydrate bioavailability. D_G [mg/kg/min] represents the intake of carbohydrates per kg of body weight.

A.3 Subcutaneous insulin absorption model

The model employs a linear model of subcutaneous insulin absorption

$$\dot{I}(t) = -k_e I(t) + \frac{S_2(t)}{V_I t_I}, \tag{A.3a}$$

$$\dot{S}_1(t) = u_1(t) - \frac{S_1(t)}{t_I}, \tag{A.3b}$$

$$\dot{S}_2(t) = \frac{S_1(t) - S_2(t)}{t_I}, \tag{A.3c}$$

where k_e [min^{-1}] describes the insulin clearance from plasma, u_1 [μU/kg/min] is the subcutaneous insulin infusion rate, V_I [mL/kg] is the distribution volume of plasma

insulin, and t_I [min] is the insulin absorption time constant. $S_1(t)$ [μU/kg] and $S_2(t)$ [μU/kg] represent a two-compartment absorption model of subcutaneously administered insulin.

A.4 Subcutaneous glucagon absorption model

Herrero *et al.* use the same model structure as in case of insulin to model the subcutaneous glucagon absorption

$$\dot{N}(t) = -k_N N(t) + \frac{Z_2(t)}{V_N t_N}, \tag{A.4a}$$

$$\dot{Z}_1(t) = u_2(t) - \frac{Z_1(t)}{t_N}, \tag{A.4b}$$

$$\dot{Z}_2(t) = \frac{Z_1(t) - Z_2(t)}{t_N}. \tag{A.4c}$$

$u_2(t)$ [pg/kg/min] is the glucagon infusion rate per body weight. $Z_1(t)$ [pg/kg] and $Z_2(t)$ [pg/kg] represent a two-compartment absorption of subcutaneously administered glucagon.

A.5 Model parameters

In our simulations, we use separate sets of time-varying parameters originally identified from 3 patients to reproduce the circadian rhythm. Three time windows, where each time window contains a major meal (breakfast, lunch or dinner), are considered: 18:00 - 05:00, 05:00 - 12:00, and 12:00 - 18:00. The following parameters vary between the three considered time windows: The insulin sensitivity, S_I, the glucagon sensitivity, S_N, the time constant, t_G, and the two parameters, p_2 and p_3. We use the model together with the identified time-varying parameters to compare the performance of the different prediction models.

A.6 Glucose measurement

A CGM provides measurements to the controller. The sensor measures glucose concentration in the interstitial tissue, which differs from the glucose concentration in the plasma. We use a model that relates the plasma glucose concentration, G [mg/dL], to the interstitial glucose concentration, G_{sub} [mg/dL], and a non-Gaussian noise model to simulate noise in the signal from the CGM. Hence, the model to describe the CGM signal consists of two parts. The first part describes the transport of glucose in the blood (plasma) to the interstitial tissues. This part of the model is

$$\frac{dG_{sub}}{dt} = \frac{1}{\tau_{sub}} \left(G(t) - G_{sub}(t) \right). \tag{A.5}$$

$G_{sub}(t)$ is the interstitial glucose concentration and $G(t)$ is the blood glucose concentration. The time constant, τ_{sub}, is associated with glucose transport from blood to interstitial tissues.

The second part of the model to describe the CGM signal is the non-Gaussian sensor noise. This part of the model is given by

$$e_k = 0.7(e_{k-1} + v_k), \ k \geq 1, \tag{A.6a}$$

$$v_k \sim N_{iid}(0, 1), \tag{A.6b}$$

$$\eta_k = \xi + \lambda \sinh\left(\frac{e_k - \gamma}{\delta} \right), \tag{A.6c}$$

Table A.1. Parameters of the insulin and glucagon absorption.

Parameter	Patient 1	Patient 2	Patient 3
k_e (min^{-1})	0.1300	0.1300	0.1500
t_I (min)	59.178	74.900	71.496
V_I (ml/kg)	124.92	71.210	121.80
I_b (μU/ml)	8.6935	15.274	8.3832
k_N (min^{-1})	0.2000	0.2141	0.3771
t_N (min)	30.274	14.850	19.795
V_N (ml/kg)	255.11	250.00	230.67
N_b (pg/ml)	47.465	48.298	59.391

and the initial condition $e_0 \sim N_{iid}(0, 1)$. The parameters are listed in Breton and Kovatchev (2008).

The glucose value, G_{CGM} [mg/dL], returned by the sc CGM that is used for the controller feedback is

$$G_{CGM}(t_k) = G_{sub}(t_k) + \eta_k. \tag{A.7}$$

A.7 Parameters of the simulation model

Upon a consultation with the authors, the simulation model parameters presented in Herrero et al. (2013) have been reidentified due to very small distribution volumes in the original paper as reported in Table A.1. The parameters $S_G = 0.014$ min^{-1}, $V = 1.7$ dl/kg and $A_g = 0.9$ remain the same as in Herrero et al. (2013).

REFERENCES

Bátora, V., Tárnik, M., Murgaš, J., Schmidt, S., Nørgaard, K., Poulsen, N.K., Madsen, H., Boiroux, D., and Jørgensen, J.B. (2015). The contribution of glucagon in an artificial pancreas for people with type 1 diabetes. In *2015 American Control Conference (ACC 2015)*, 5097–5102.

Bátora, V., Tárnik, M., Murgaš, J., Schmidt, S., Nørgaard, K., Poulsen, N.K., Madsen, H., and Jørgensen, J.B. (2014). Bihormonal model predictive control of blood glucose in people with type 1 diabetes. In *2014 IEEE Multi-Conference on Systems and Control (MSC)*, 1693 – 1698.

Bemporad, A. and Morari, M. (1999). Control of systems integrating logic, dynamics, and constraints. *Automatica*, 35(3), 407–427.

Boiroux, D., Finan, D.A., Poulsen, N.K., Madsen, H., and Jørgensen, J.B. (2010). Nonlinear model predictive control for an artificial β-cell. In *Recent Advances in Optimization and its Applications in Engineering*, 299 – 308. Springer.

Boiroux, D., Bátora, V., Hagdrup, M., Tárnik, M., Murgaš, J., Schmidt, S., Nørgaard, K., Poulsen, N.K., Madsen, H., and Jørgensen, J.B. (2015). Comparison of prediction models for a dual-hormone artificial pancreas. *IFAC-PapersOnLine*, 48(20), 7–12.

Boiroux, D., Duun-Henriksen, A.K., Schmidt, S., Nørgaard, K., Madsbad, S., Poulsen, N.K., Madsen, H., and Jørgensen, J.B. (2018). Overnight glucose control in people with type 1 diabetes. *Biomedical Signal Processing and Control*, 39, 503–512.

Boronat, M., Sánchez-Hernández, R.M., Rodríguez-Cordero, J., Jiménez-Ortega, A., and Nóvoa, F.J. (2015). Suspension of basal insulin to avoid hypoglycemia in type 1 diabetes treated with insulin pump.

Endocrinology, Diabetes & Metabolism Case Reports, 2015.

Breton, M. and Kovatchev, B. (2008). Analysis, modeling, and simulation of the accuracy of continuous glucose sensors. *Journal of Diabetes Science and Technology*, 2, 853–862.

Castle, J.R., Yuen, K.C.J., Engle, J.M., Kagan, R., Youssef, J.E., Ward, W.K., and Massoud, R.G. (2010). Novel use of glucagon in a closed-loop system for prevention of hypoglycemia in type 1 diabetes. *Diabetes Care*, 33(6), 1282 – 1287.

Castle, J.R., Youssef, J.E., Branigan, D., Newswanger, B., Strange, P., Cummins, M., Shi, L., and Prestrelski, S. (2016). Comparative pharmacokinetic/pharmacodynamic study of liquid stable glucagon versus lyophilized glucagon in type 1 diabetes subjects. *Journal of Diabetes Science and Technology*, 10(5), 1101–1107.

Dua, V., Bozinis, N.A., and Pistikopoulos, E.N. (2002). A multiparametric programming approach for mixed-integer quadratic engineering problems. *Computers & Chemical Engineering*, 26(4), 715–733.

El Youssef, J., Castle, J.R., Bakhtiani, P.A., Haidar, A., Branigan, D.L., Breen, M., and Ward, W.K. (2014). Quantification of the glycemic response to microdoses of subcutaneous glucagon at varying insulin levels. *Diabetes Care*, 37(11), 3054–3060.

Hagdrup, M., Boiroux, D., Mahmoudi, Z., Madsen, H., Poulsen, N.K., Poulsen, B., and Jørgensen, J.B. (2016). On the significance of the noise model for the performance of a linear MPC in closed-loop operation. *IFAC-PapersOnLine*, 49(7), 171–176.

Haidar, A. (2016). The artificial pancreas - how closed-loop control is revolutionizing diabetes. *IEEE Control Systems Magazine*, 36(5), 28–47.

Haidar, A., Legault, L., Messier, V., Mitre, T.M., Leroux, C., and Rabasa-Lhoret, R. (2015). Comparison of dual-hormone artificial pancreas, single-hormone artificial pancreas, and conventional insulin pump therapy for glycaemic control in patients with type 1 diabetes: an open-label randomised controlled crossover trial. *The Lancet Diabetes and Endocrinology*, 3(1), 17–26.

Haidar, A., Messier, V., Legault, L., Ladouceur, M., and Rabasa-Lhoret, R. (2017). Outpatient 60-hour day-and-night glucose control with dual-hormone artificial pancreas, single-hormone artificial pancreas, or sensor-augmented pump therapy in adults with type 1 diabetes: an open-label, randomised, crossover, controlled trial. *Diabetes, Obesity and Metabolism*. DOI:10.1111/dom.12880.

Herrero, P., Georgiou, P., Oliver, N., Reddy, M., Johnston, D., and Toumazou, C. (2013). A Composite Model of Glucagon-Glucose Dynamics for In Silico Testing of Bihormonal Glucose Controllers. *Journal of Diabetes Science and Technology*, 7(4), 941–951.

Hovorka, R., Canonico, V., Chassin, L.J., Haueter, U., Massi-Benedetti, M., Federici, M.O., Pieber, T.R., Schaller, H.C., Schaupp, L., Vering, T., and Wilinska, M.E. (2004). Nonlinear model predictive control of glucose concentration in subjects with type 1 diabetes. *Physiological Measurement*, 25, 905–920.

Jørgensen, J.B., Huusom, J.K., and Rawlings, J.B. (2011). Finite horizon MPC for systems in innovation form. In *50th IEEE Conference on Decision and Control and European Control Conference (CDC-ECC 2011)*, 1896 – 1903.

Man, C.D., Micheletto, F., Lv, D., Breton, M., Kovatchev, B., and Cobelli, C. (2014). The UVa/Padova type 1 diabetes simulator: new features. *Journal of Diabetes Science and Technology*, 8(1), 26–34.

Mhaskar, P., El-Farra, N.H., and Christofides, P.D. (2005). Predictive control of switched nonlinear systems with scheduled mode transitions. *IEEE Transactions on Automatic Control*, 50(11), 1670–1680.

Reiter, M., Reiterer, F., and del Re, L. (2016). Bihormonal glucose control using a continuous insulin pump and a glucagon-pen. In *European Control Conference (ECC)*, 2435–2440.

Rossetti, P., Ampudia-Blasco, F.J., Laguna, A., Revert, A., Vehì, J., Ascaso, J.F., and Bondia, J. (2012). Evaluation of a novel continuous glucose monitoring-based method for mealtime insulin dosingthe ibolusin subjects with type 1 diabetes using continuous subcutaneous insulin infusion therapy: a randomized controlled trial. *Diabetes Technology & Therapeutics*, 14(11), 1043–1052.

Russell, S.J., El-Khatib, F.H., Nathan, D.M., Magyar, K.L., Jiang, J., and Damiano, E.R. (2012). Blood glucose control in type 1 diabetes with a bihormonal bionic endocrine pancreas. *Diabetes Care*, 35(11), 2148–2155.

Russell, S.J., El-Khatib, F.H., Sinha, M., Magyar, K.L., McKeon, K., Goergen, L.G., Balliro, C., Hillard, M.A., Nathan, D.M., and Damiano, E.R. (2014). Outpatient glycemic control with a bionic pancreas in type 1 diabetes. *New England Journal of Medicine*, 371(4), 313–325.

Srinivasan, A., Lee, J.B., Dassau, E., and Doyle III, F.J. (2014). Novel insulin delivery profiles for mixed meals for sensor-augmented pump and closed-loop artificial pancreas therapy for type 1 diabetes mellitus. *Journal of diabetes science and technology*, 8(5), 957–968.

Trevitt, S., Simpson, S., and Wood, A. (2015). Artificial pancreas device systems for the closed-loop control of type 1 diabetes: What systems are in development? *Journal of Diabetes Science and Technology*, 10(3), 714–723.

Wendt, S.L., Møller, J.K., Haidar, A., Knudsen, C.B., Madsen, H., and Jørgensen, J.B. (2016). Modelling of glucose-insulin-glucagon pharmacodynamics in man. In *38th Annual International Conference of the IEEE Engineering in Medicine and Biology Society (EMBS 2016)*.

Wendt, S.L., Ranjan, A., Møller, J.K., Schmidt, S., Knudsen, C.B., Holst, J.J., Madsbad, S., Madsen, H., Nørgaard, K., and Jørgensen, J.B. (2017). Cross-validation of a glucose-insulin-glucagon pharmacodynamics model for simulation using data from patients with type 1 diabetes. *Journal of Diabetes Science and Technology*. DOI:10.1177/1932296817693254.

Zealand Pharma - Dasiglucagon multiple-dose pump use (2018). Website: http://www.zealandpharma.com/portfolio/glucagon-multiple-dose-version-zp4207.